Proc. Natl. Acad. Sci. USA
Vol. 90, pp. 9315–9319, October 1993
Biochemistry

Multiple nucleosome positioning with unique rotational setting for the *Saccharomyces cerevisiae* 5S rRNA gene *in vitro* and *in vivo*

MEMMO BUTTINELLI*, ERNESTO DI MAURO*†, AND RODOLFO NEGRI*

*Centro Acidi Nucleici, Consiglio Nazionale delle Ricerche, and †Fondazione "Istituto Pasteur–Fondazione Cenci Bolognetti" c/o Dipartimento di Genetica e Biologia Molecolare, Università di Roma La Sapienza P.le A.Moro 5, 00185 Rome, Italy

Communicated by K. van Holde, June 14, 1993

ABSTRACT **A simple no-background assay was developed for high-resolution *in vivo* analysis of yeast chromatin. When applied to *Saccharomyces cerevisiae* 5S rRNA genes (5S rDNA), this analysis shows that nucleosomes completely cover this chromosomal region, occupying alternative positions characterized by a unique helical phase. This supports the notion that sequence-intrinsic rotational signals are the major determinant of nucleosome localization. Nucleosomal core particles reconstituted *in vitro* occupy the same positions and have the same helically phased distribution observed *in vivo*, as determined by mapping of exonuclease III-resistant borders, mapping by restriction cleavages, and by DNase I and hydroxyl-radical digestion patterns.**

Nucleosomes have long been considered as general repressors of chromatin function. Their active role in transcription is now emerging (1), possibly related to functions of topological organization of chromatin in promoter regions (2). Therefore, understanding the rules that govern localization and stability of nucleosomes is of major relevance.

The specific location of a nucleosomal core particle (NCP) on DNA is attained through the interaction of the histone proteins with an ensemble of rotational and translational signals intrinsic to the DNA sequence (3, 4). The relative contribution of these parameters and the function of other factors (boundary or domain effects, ancillary proteins, cooperativity, etc.; refs. 5 and 6) are open problems.

Rotational phases on DNA are determined by a repetition of bendability signals due to particular combinations of base pairs (7, 8). These sequence elements repeat themselves with the same periodicity as the DNA helical repeat, define a permissive rotational phase, and favor the deposition of a NCP onto a defined side of the double strand. DNA sequences with strong rotational signals are expected to favor occupancy by multiple, helically phased NCPs. In contrast, translational signals would favor unique occupancies. Examples of specific nucleosome positioning sequences are known, both *in vitro* (9–11) and *in vivo* (refs. 12–14; reviewed in ref. 15). The nature of the translational signals for nucleosome positioning remains elusive.

We report that on *Saccharomyces cerevisiae* 5S repeat genes *in vivo*, nucleosomes occupy multiple, helically phased positions. This finding supports the notion that at least for these genes the rotational information is the major determinant for NCP localization, both *in vitro* and *in vivo*. It also implies that each individual NCP can choose among several quasi-isoenergetic positions (a phenomenon that may have important biological implications). The fact that the same multiplicity of positions, coupled with uniqueness of rotational phase, can be detected *in vivo* implies that genes exist on which nucleosomes form on multiple positions and/or enjoy facilitated rotational displacements.

The publication costs of this article were defrayed in part by page charge payment. This article must therefore be hereby marked "*advertisement*" in accordance with 18 U.S.C. §1734 solely to indicate this fact.

MATERIALS AND METHODS

Materials. T4 polynucleotide kinase was from United States Biochemical; Klenow DNA polymerase, exonuclease III, DNase I, restriction endonucleases, and micrococcal nuclease (MN) were from Boehringer Mannheim or New England Biolabs; *Taq* DNA polymerase was from Promega; radiochemicals were from NEN, and nystatin was from Sigma.

DNA Segments. The DNA segments used were (*a*) the 305-bp *Eco*RI–*Hin*dIII fragment of the pBB111F plasmid (16) containing a single copy of the yeast 5S rDNA repeat gene, with the first adenine of the *Eco*RI site being position 1; (*b*) a 312-bp PCR product, the same as *a* but starting 2 bp upstream of the *Eco*RI site; and (*c*) a 280-bp PCR product spanning positions 20 to 299. For 3′- and 5′-terminal labeling according to standard procedures, plasmid DNA was linearized by restriction enzyme digestion, labeled, and digested with a secondary restriction enzyme. The restriction fragments were separated in agarose and the band of interest was recovered. Internally labeled DNAs *b* and *c* were produced by 30-cycle PCR synthesis in the presence of [α-^{32}P]dATP (dATP/[α-^{32}P]dATP molar ratio was 500).

Hydroxyl Radical Analysis. This procedure has been described (17). Cutting conditions were as follows: 12.5 μM $(NH_4)_2Fe(SO_4)_2$, 25 μM EDTA, 0.0375% H_2O_2, 20 mM NaCl, 4 mM Tris·HCl (pH 8.0), 1 μg of nonspecific DNA, and 800 ng of radioactive reconstituted NCP were incubated (80 μl) at 20°C from 0.5 to 4 min.

Reconstitution of NCPs. This was done according to the salt dilution protocol (8), going from 1 M NaCl to 100 mM NaCl. The NCPs were from chicken erythrocytes (18). Reconstitution was performed at various molar ratios between NCPs and acceptor DNA (Fig. 1), with a DNA concentration $\geq$ 10 μg/ml, and was monitored by electrophoresis in 0.75% (wt/vol) agarose in 0.5× TBE buffer (45 mM Tris/45 mM boric acid/1 mM EDTA) and evaluated by densitometry.

***In Vivo* Chromatin Analysis.** Haploid yeast W303-1a (*MATa ade2-1 ura3-1 his3-11,15 trp1-1 leu2-3,112 can1-100*) (from R. Sternglanz, State University of New York at Stony Brook) was grown to 1–5 × 10^7 cells per ml. Spheroplasts (19) were washed with 1 M sorbitol and suspended (1–5 × 10^7 per ml) in 1 M sorbitol/20 mM Tris·HCl, pH 8/50 mM NaCl/1.5 mM $CaCl_2$ with nystatin at 30 μg/ml. These conditions allow penetration of MN into the spheroplasts and digestion of chromatin in the absence of lysis (S. Venditti and G. Camilloni, personal communication). MN was added at 20 units/ml, or as otherwise indicated; after 15 min at 37°C, the reaction was stopped with 5 mM EGTA. Spheroplasts were digested with proteinase K in 0.2% SDS and extracted three times with phenol/chloroform/isoamyl alcohol, 24:24:1 (vol/vol). Resuspended samples were electrophoresed in a 1.5% agarose gel to resolve the nucleosomal DNA ladder. Monomeric DNA was eluted, treated with phosphatase, labeled at

Abbreviations: MN, micrococcal nuclease; NCP, nucleosomal core particle.

low specific activity with kinase (see Fig. 3), and run in denaturing polyacrylamide gels to remove internally nicked monomeric molecules. Full-length denatured monomeric DNAs were recovered, purified, and used in multiple cycles of primer extension by *Taq* polymerase with a 5′-labeled oligonucleotide primer (see Fig. 3), thus locating the borders of the monomer-length MN digestion products (the *in vivo* protected nucleosomal DNA) that contained the indicated oligonucleotide primers.

RESULTS

Preferential Reconstitution of Monomer NCPs on the 305-bp Fragment Containing the 5S rRNA Gene. Reconstituted NCPs were analyzed by agarose gel electrophoresis in a band-retardation assay (Fig. 1*A*). A single type of complex was preferentially formed, which was extracted from the agarose gel and extensively digested with MN; the size of the protected DNA fragment was 146 ± 2 bp (data not shown), indicating that the major product was a bona fide monomeric core particle (6). Reconstituted NCPs obtained with yeast or chicken erythrocyte donor NCPs have the same size, 146 bp (20). Minor amounts of dimeric particles also formed (Fig. 1*A*). On a DNA fragment of 305 bp, the formation of a second NCP is disfavored because the second particle would occupy <14 helical repeats (except for the NCPs that form at the side of NCPs 1 and 16; Fig. 1*D*). The second NCP would overhang the DNA to various extents, at the expense of its stability.

Sixteen NCPs Form *in Vitro* in Alternative Locations on the 5S Fragment. *Exonuclease III analysis.* Exonuclease III digestion of the monomeric NCPs (Fig. 1 *B–D*) reveals multiple borders (lanes 5–8 in Fig. 1 *B* and *C*) that belong to a *monomeric* particle because (*i*) a second NCP forms on the same DNA fragment only with difficulty (see Fig. 1*A*) and (*ii*) due to its processive nature, the exonuclease III assay reveals only the border of the first NCP (the border of a hypothetical second NCP being hidden by the first one). The borders identified here have a good "upper strand/lower strand" match of 146 ± 2 bp (a reliable indication that the borders refer to a defined NCP; ref. 21). The 16 matches (numbered in Fig. 1*D*) encompass the entire DNA segment. The borders are of different intensities. Groups of strong borders are distributed all over the fragment and are separated by groups of weak borders, revealing the formation of a quasi-homogeneous population of NCPs with affinity for the whole sequence. The more frequent NCPs are nos. 4–7 and 11–13.

Mapping by MN and restriction endonucleases. Four evenly distributed cleavage sites map on the 5S fragment (Fig. 1*D*) (22). Uniformly labeled DNA *c* was reconstituted and the monomeric complex was digested with MN. The resulting 146 ± 2-bp fragments were purified through non-denaturating polyacrylamide gel electrophoresis and digestion with one of the four restriction enzymes. The number and the size of the DNA fragments produced verify whether the upper strand/lower strand matches determined by exonuclease III (Fig. 1*D*) are correct. The experiment (Fig. 2)

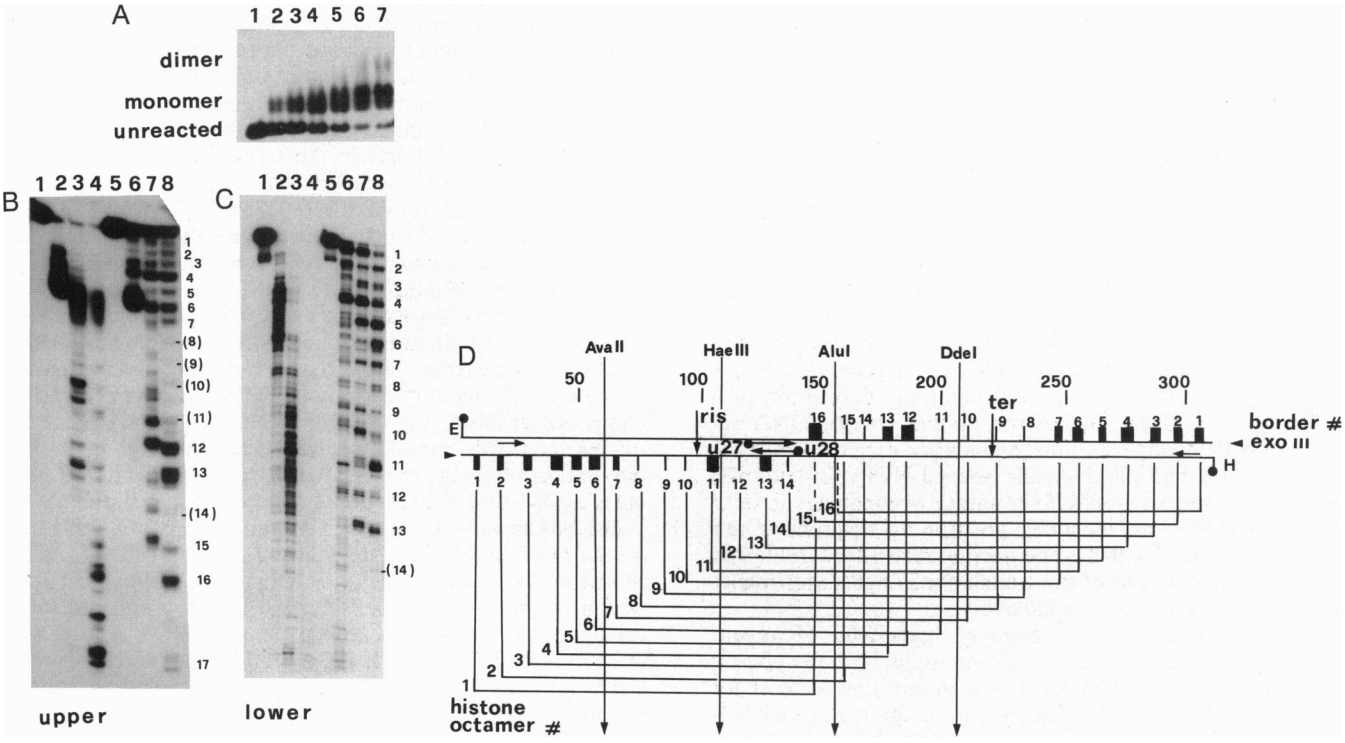

FIG. 1. Reconstitution and exonuclease III analysis of NCPs on the 305-bp fragment containing 5S rDNA. (*A*) NCPs were reconstituted on 800 ng (50,000 cpm) of 5′-end-labeled 5S DNA (fragment *a*) at donor chicken erythrocyte NCPs/labeled DNA molar ratios of 0, 5, 10, 20, 40, 80, and 160 (lanes 1–7). (*B* and *C*) Exonuclease III digestion of NCPs reconstituted with 5′-end-labeled upper or lower strand, respectively. Exonuclease III treatment (150 units/ml, 30°C for 0, 2, 10, or 40 min in 100 μl of 20 mM Tris·HCl, pH 8.0/2 mM $MgCl_2$/50 mM NaCl/0.01% Nonidet P-40) was carried out on 10,000 cpm of 5′-end-labeled DNA (lanes 1–4) or of monomer NCP (same sample as in lane 5 of *A*) (lanes 5–8). Size markers are not shown. Exonuclease III borders are numbered; numbers in parentheses refer to weak borders. (*D*) Localization of the reconstituted NCPs. The exonuclease III borders (from *B* and *C*) are indicated by filled rectangles (whose size is proportional to the intensity of the bands) or by lines (weak borders). Dots indicate the labeled extremities (E, *Eco*RI; H, *Hin*dIII), triangles show the direction of exonuclease III digestion, and the two arrows represent the oligonucleotides used to generate DNA *c* by PCR. The RNA initiation (ris) and termination (ter) sites of the 5S gene, the restriction sites used for the experiment of Fig. 2, and the U27 and U28 oligonucleotides used for the *in vivo* mapping in Fig. 3 are indicated. The connecting bars indicate the region of 146 ± 2 bp putatively encompassed by a NCP. The dashed lines for the upstream border of NCPs 15 and 16 refer to uncertainty of the exonuclease III mapping of these two innermost sites.

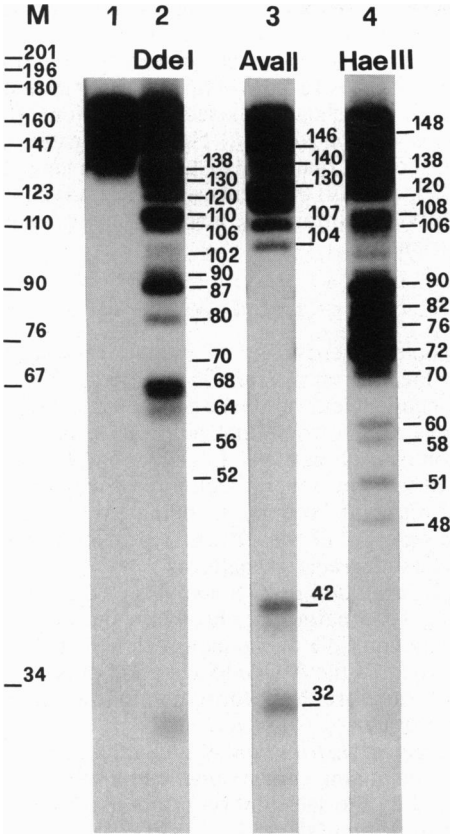

FIG. 2. Localization of the NCPs by restriction mapping. NCPs were reconstituted on 3 μg (10,000 cpm) of homogeneously labeled DNA *c* as in lane 5 of Fig. 1*A* and digested with MN (10 min, 37°C, 2 units/ml in 20 mM Tris·HCl, pH 8/1.5 mM $CaCl_2$/50 mM NaCl/0.01% Nonidet P-40). After proteinase K and phenol treatment, the protected DNA fragments were purified in a 6% polyacrylamide gel (with Tris/borate/EDTA buffer) and digested with restriction enzyme as indicated (2500 cpm per sample) (lanes 2–4). Lane 1, undigested fragment. Electrophoresis was in nondenaturing 10% polyacrylamide (Tris/borate/EDTA buffer). See Table 1. *Msp* I fragments of pBR322 provided size markers (M, lengths in base pairs).

consists of reconstitution, digestion by MN, isolation of the protected fragments, digestion by restriction endonuclease, and electrophoresis. The DNA is homogeneously labeled; therefore the intensities of the bands are proportional to their size. The procedure, the technical problems, and the logic of this experiment have been discussed (23). The observed sizes (Fig. 2 and Table 1) correspond to the sizes of the fragments expected from the scheme in Fig. 1*D*. The expectation is based on how many exonuclease III-mapped NCPs would be cleaved by each restriction enzyme and on the expected size of the cleavage products. Fig. 2 shows that the prediction is respected. DNA *b* was also tested, with the same results (not shown). In conclusion, the results of exonuclease III analysis (i.e., the localization of NCPs on multiple, helically-phased sites) are confirmed by this independent assay, ruling out possible artifacts of the exonuclease III assay (such as strand invasion).

NCP mapping by hydroxyl-radical degradation. Nucleosomes have been mapped by protection against degradation with hydroxyl radicals (17). When performed on monomeric NCPs formed on 5S DNA, this analysis reveals the helical periodicity of the protection (data not shown). This lends further support to the fact that we are dealing with bona fide core particles, provides information on the helical periodicity of the exposure of DNA in these NCPs, and shows that the whole DNA fragment is covered with NCPs, from one extremity to the other. The cleavage periodicity observed spans the whole fragment. This can occur only in the case of helical-phase-wise distributed multiple NCPs. In fact, randomly distributed particles would obscure periodicity, and a single or a small family of localized particles would not cover the whole DNA fragment.

DNase I footprinting. In the case of uniquely localized nucleosomes, a 140- to 150-bp-long area of protection against DNase I attack, with protected sites spaced by 10 bp, is expected (19). In the case of particles distributed on alternative positions, a protection whose intensity is proportional to the number of NCPs that form on it should be observed. Therefore, in our case an area of protection is expected with the highest intensity on the central part of the DNA segment. Indirect DNase I footprint data for the monomer isolated from the gel show a perturbation of the cleavage rate from position 120 to position 210 (data not shown). The results of DNase I protection confirm the multiple, helically-phased occupancy of the DNA segment by NCPs.

Nucleosomes Occupy *in Vivo* the Same Multiple, Helically Phased Sites Occupied *in Vitro*. A MN digest of nystatin-permeabilized cells (Fig. 3) localizes nucleosomes on *in vivo* chromatin. Nystatin-treated spheroplasts were digested with MN, DNA was extracted and run through a preparative agarose gel, monomer-length DNA was isolated from the typical MN digestion ladder, purified, labeled at low specific activity to allow quantitative handling, and run in a denaturing polyacrylamide gel (to separate monomer-sized DNA from internally nicked molecules) (lanes 5 and 7). Primer extension was performed on these full-length molecules by using one of two high-specific-activity oligonucleotide primers (U27 and U28, complementary and oppositely oriented; see map in Fig. 1), the size of the products was determined (lanes 6 and 8), and the products were mapped. In the

Table 1. NCP localization by restriction mapping

Dde I		*Ava* II		*Hae* III	
Expected	Observed	Expected	Observed	Expected	Observed
102 + 48	106 + 52	144 + 6	146	148 + 3	148
92 + 57	90 + 64	138 + 14	140	142 + 12	138
83 + 68	87 + 68	126 + 20	130	126 + 21	120
72 + 77	80 + 70	110 + 31	107 + 32	115 + 31	108
110 + 40	110	102 + 42	104 + 42	93 + 50	90
52 + 100	102 + 56			79 + 58	76
44 + 110	110			71 + 66	72
28 + 118	120			78 + 60	72
18 + 128	130			90 + 52	82
5 + 138	138			100 + 42	106

Values are restriction fragment lengths in base pairs. In each case the expected length was observed. Autoradiograms (various exposures) were scanned. See Fig. 2.

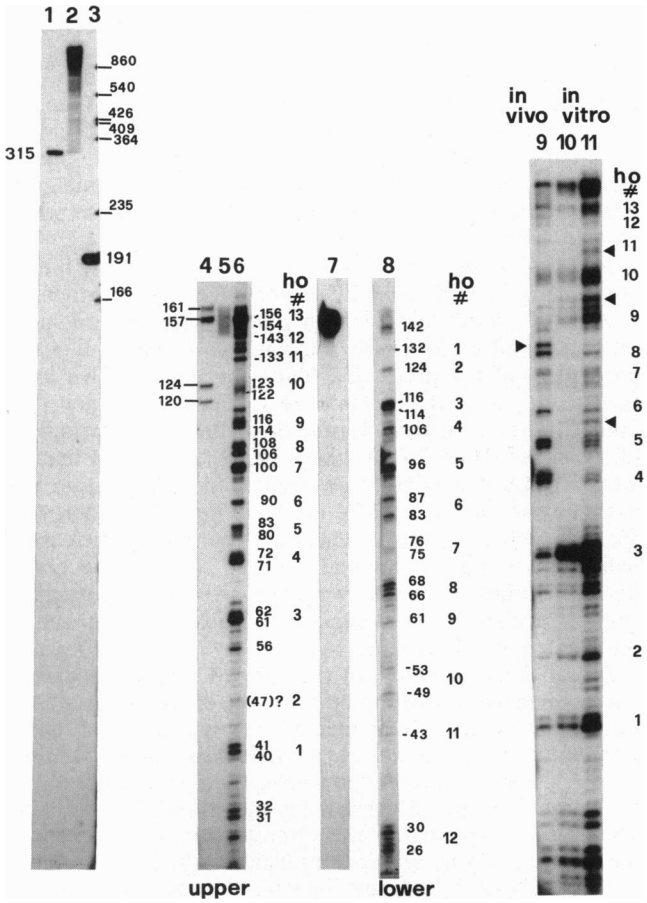

FIG. 3. Localization of nucleosome positions in cellular chromatin by MN digestion and primer extension of the resulting products. Lanes 1–3, controls of the primer extension reaction, show that on this DNA, with these oligonucleotides and under the conditions used, there is no primer extension-induced background or sequence-induced pausing. Lane 1, 100 ng of yeast genomic DNA purified from nystatin-treated spheroplasts (no MN, 15 min, 37°C), *Hpa* II-cleaved; primer extension, 30 cycles with U27 oligonucleotide (U27 and U28 are the oppositely oriented 20-mers used for mapping the MN digest of the 5S region, spanning bp 118–137; see Fig. 1); lane 2, 1 μg of yeast genomic DNA purified from spheroplasts treated as above, primer-extended with U27, no restriction enzyme; lane 3, 5 ng of pBB111F plasmid DNA, cut with *Hin*dIII and primer-extended with U27 as above. The size of the resulting amplification fragments (lanes 1 and 3) is as expected (24); lane 4, size markers (*Dde* I fragments of pSP65; smaller markers used are not shown); lane 5, 200 ng of monomer DNA (150–158 bp) after low-specific-activity labeling and purification; lane 7, same as lane 5, but with 1 μg of the DNA (from this heavily loaded lane, it is evident that no internal breakages are present); lane 6, 200 ng of the DNA shown in lane 5 after 30 cycles of primer extension with U27; lane 8, same, after 30 cycles with U28. Primer extension conditions: 30 cycles (90 sec at 94°C, denaturation; 120 sec at 65°C, annealing; 120 sec at 72°C, elongation); oligonucleotide, 0.2 pmol, 1.5 μCi/pmol (1 μCi = 37 GBq). Products were purified by extraction with phenol/chloroform/isoamyl alcohol, 24:24:1, and analyzed by electrophoresis in 8% polyacrylamide under denaturing conditions. Lanes 9–11 show direct comparison of the localization of *in vivo* and *in vitro* NCPs. Lane 9, *in vivo*, 200 ng of core-monomer DNA (144–148 bp) prepared by extensive MN digestion (200 units/ml, 37°C, 15 min) (25) of nystatin-treated spheroplasts, purified and primer-extended as above; lanes 10 and 11, *in vitro*, 1 and 2 ng of core-monomer DNA prepared as in Fig. 2, lane 1, purified in a denaturing gel and primer-extended with U27 as above. ho, Histone octamer.

primer-extension conditions chosen (G+C-rich oligonucleotides and a high annealing temperature, 65°C), no background due to abortive elongation or pausing was produced (lanes 1–3). Lanes 6 and 8 show the MN cleavages on both strands. The numbers refer to the cleavage positions *in vivo*.

Direct comparison of the MN pattern *in vivo* (Fig. 3, lane 9) and *in vitro* (lanes 10 and 11) for the upper strand shows (*i*) multiplicity and helically phased distribution of cleavages both *in vivo* and *in vitro*, (*ii*) cleavages on the same sites (therefore showing that NCP distribution *in vivo* and *in vitro* is the same), and (*iii*) differences in the relative intensity for several cleaved positions; the major differences are indicated by filled triangles.

DISCUSSION

NCPs completely cover the 5S gene-containing DNA segment and localize on alternative positions. The alternative multiple occupancies are spaced by one helical repeat, showing that one unique rotational phase is responsible for the localization of each particle. Localization of the NCPs was obtained *in vitro* by several techniques: mapping of exonuclease III-resistant borders, mapping by restriction cleavages, and analysis of the DNase I protection and the hydroxyl-radical degradation patterns.

The high-resolution *in vivo* analysis of the distribution of the MN digestion pattern of chromatin shows that the same property (the multiple occupancy with helically phased distribution) governs the *in vivo* localization of nucleosomes on this DNA. Therefore, NCP formation follows the same rules *in vivo* and *in vitro*.

(*i*) *Equilibrium distribution*. We have observed that identical NCP positioning can be obtained by salt-dialysis reconstitution and by the salt-dilution protocol (as determined by exonuclease III and DNase I analysis). As pointed out (23), the fact that the same positions are obtained by different kinetic pathways indicates that we are dealing with an equilibrium distribution of positioned nucleosomes. We have also determined (by exonuclease III analysis; data not shown) that the NCP distribution is independent of the histone/DNA input ratio. This further supports the idea that the multiple positioning is an equilibrium distribution, homogeneous and continuous over the DNA fragment tested.

(*ii*) *Curved DNA and nucleosomes*. Multiple nucleosome positions occur on synthetic (21), natural (20, 26–28), and engineered repetitive (25) DNAs; the occurrence of the same phenomenon *in vivo* in animal viruses was suggested (29). Multiple positions correlate with intrinsic curvature (20, 21, 26, 27); the phased repetitions of certain sequence elements induce strong bending in the *Crithidia fasciculata* kinetoplast DNA and preferentially attract and phase histone octamers on multiple positions with a unique rotational phasing (20). The fact that the average repetition of both these sequence elements and of the phased NCPs occurs every 10.26 bp (20) shows a cause–effect relationship between curvature and preferential deposition of NCPs. Furthermore, linkage reduction (i.e., writhing) favors nucleosome formation in large (30), small (31), and micro (32) domains. The bent character of the 5S rDNA that rotationally phases NCPs (ref. 22 and this work) has been described (23). In conclusion, sequence-intrinsic and supercoil-induced curvatures attract and helically orient NCPs.

(*iii*) *Rotational displacements*. Minor positions of nucleosomes on 5S rDNA have been reported (23), indicating that generation of multiple positions is an inherent property of the 5S rDNA. The mobility of nucleosomes on these sequences (33, 34) is presumably a consequence of this property. In multiple occupancies by NCPs the free-energy differences between major and minor positions are small (<1 kcal/mol) (21, 23), suggesting that changes in nucleosome positioning are obtained by shifting from one permissive position to the next along the same rotational phase (i.e., the same side). The absence of randomly positioned nucleosomes favors this

model. Other alternatives [namely, change in position through the high-energy-requiring detachment and rebinding (21) or through translational sliding] are less probable.

Taken together, the observation that the equilibrium distribution of nucleosomes on intrinsic or supercoil-induced curvatures may undergo low-energy-requiring displacements supports the idea that during genetic processes, nucleosome dynamics follows simple rotationally determined rules. On intrinsically curved sequences, the multiple localizations and the alternatives among quasi-isoenergetic positions are a potential regulatory phenomenon.

Transcription of 5S genes requires binding of transcription factors TFIIIA, -B, and -C (35). Yeast 5S RNA genes engaged in transcription complexes are continuously protected from cleavage by DNase I (16). These complexes span more than 160 bp and might also possess a convoluted tridimensional structure (36). Bridging interactions between the TFIII (C·A)–DNA complex and TFIIIB have been shown to depend on binding of TFIIIA to DNA (37). *Xenopus* TFIIIA binds to homologous 5S genes reconstituted *in vitro* with chicken erythrocyte NCPs even when its binding site on DNA is partially overlapping an NCP (ref. 11; but see also ref. 38). Therefore, TFIIIA may bind to a DNA–histone octamer complex in which the rotational setting on DNA is the dominant parameter allowing the correct exposure of the relevant DNA sequences.

The TFIIIA binding region is centrally located on the group of histone octamers whose intensity decreases *in vivo* (nos. 9–13) and is laterally located on the octamer whose intensity increases (nos. 4–8), thus suggesting a possible role of TFIIIA in modulating the *in vivo* localization and frequency of nucleosomes.

Thanks are due to Lucia DiMarcotullio and Kelly P. Williams for discussions. This work was supported by Programma Finalizzato Biotecnologie (Consiglio Nazionale delle Ricerche) and Ingegneria Genetica.

1. Van Holde, K. (1993) *Nature (London)* **362,** 111–112.
2. Schild, C., Claret, F. X., Wahli, W. & Wolffe, A. P. (1993) *EMBO J.* **12,** 423–433.
3. Satchwell, S. C. & Travers, A. A. (1989) *EMBO J.* **8,** 229–238.
4. Travers, A. A. (1989) *Annu. Rev. Biochem.* **58,** 427–452.
5. Thoma, F. & Zatchej, M. (1988) *Cell* **55,** 945–953.
6. Fedor, M. J., Lue, N. F. & Kornberg, R. D. (1988) *J. Biol. Mol.* **204,** 109–127.
7. Trifonov, E. N. & Sussman, J. C. (1980) *Proc. Natl. Acad. Sci. USA* **77,** 3816–3820.
8. Drew, H. R. & Travers, A. H. (1985) *J. Mol. Biol.* **186,** 773–790.
9. Simpson, R. T. & Stafford, D. W. (1983) *Proc. Natl. Acad. Sci. USA* **80,** 51–55.
10. Ramsay, N. (1986) *J. Mol. Biol.* **189,** 179–188.
11. Rhodes, D. (1985) *EMBO J.* **4,** 3473–3482.
12. Piña, B., Barettino, D., Truss, M. & Beato, M. (1990) *J. Mol. Biol.* **216,** 975–990.
13. Straka, C. & Hörz, W. (1991) *EMBO J.* **10,** 361–368.
14. Shimizu, M., Roth, S. Y., Szent-Gyorgy, C. & Simpson, R. T. (1991) *EMBO J.* **10,** 3033–3041.
15. Freeman, L. A. & Garrard, W. T. (1992) *Crit. Rev. Eukaryotic Gene Expressio* **2,** 165–209.
16. Braun, B. R., Riggs, D. L., Kassavetis, G. A. & Geiduschek, E. P. (1989) *Proc. Natl. Acad. Sci. USA* **86,** 2530–2534.
17. Tullius, T. D. & Dombroski, B. A. (1985) *Science* **230,** 679–681.
18. Forte, P., Leoni, L., Sampaolese, B. & Savino, M. (1989) *Nucleic Acids Res.* **17,** 8683–8694.
19. Almer, A. & Horz, W. (1986) *EMBO J.* **5,** 2681–2687.
20. Costanzo, G., Di Mauro, E., Salina, G. & Negri, R. (1991) *J. Mol. Biol.* **216,** 363–374.
21. Shrader, T. E. & Crothers, D. M. (1989) *Proc. Natl. Acad. Sci. USA* **86,** 7418–7422.
22. Mc Mahon, M. E., Stamenkovich, D. & Petes, T. D. (1984) *Nucleic Acids Res.* **12,** 8001–8016.
23. Dong, F., Hansen, J. C. & Van Holde, K. E. (1990) *Proc. Natl. Acad. Sci. USA* **87,** 5724–5728.
24. Valenzuela, P., Bell, G. I., Maziars, F. R., De Gennaro, L. J. & Rutter, W. J. (1977) *Nature (London)* **267,** 641–643.
25. Hansen, J. C., Ausio, J., Stanik, V. H. & van Holde, K. E. (1989) *Biochemistry* **28,** 9129–9136.
26. Zhang, X. Y. & Horz, W. (1984) *J. Mol. Biol.* **176,** 105–129.
27. Linxweiler, W. & Horz, W. (1985) *Cell* **42,** 281–290.
28. Clarke, M. F., Fitzgerald, P. C., Brubaker, J. M. & Simpson, R. T. (1985) *J. Biol. Chem.* **260,** 12394–12397.
29. Ponder, B. A. J. & Crawford, L. V. (1977) *Cell* **11,** 35–49.
30. Germond, J. E., Hirt, B., Oudet, P., Gross Bellard, M. & Chambon, P. (1975) *Proc. Natl. Acad. Sci. USA* **72,** 1843–1847.
31. Zivanovic, Y., Goulet, I., Revet, B., Le Bret, M. & Prunell, A. (1988) *J. Mol. Biol.* **200,** 267–290.
32. Negri, R., Costanzo, G., Venditti, S. & Di Mauro, E. (1989) *J. Mol. Biol.* **207,** 615–619.
33. Pennings, S., Meersseman, G. & Bradbury, E. M. (1991) *J. Biol. Mol.* **220,** 101–110.
34. Meerssman, G., Penning, S. & Bradbury, E. M. (1992) *EMBO J.* **11,** 2951–2959.
35. Geiduschek, E. P. & Tocchini Valentini, G. P. (1988) *Annu. Rev. Biochem.* **57,** 873–914.
36. Braun, B. R., Kassavetis, G. A. & Geiduschek, E. P. (1992) *J. Biol. Chem.* **267,** 22562–22569.
37. Kassavetis, G. A., Braun, B. R., Nguyen, L. H. & Geiduschek, E. P. (1990) *Cell* **60,** 235–245.
38. Lee, D. Y., Hayes, J. J., Pruss, D. & Wolffe, A. P. (1993) *Cell* **72,** 73–84.